Mon. Not. R. Astron. Soc. **000**, 1–12 (2013) Printed 28 May 2014 (MN LATEX style file v2.2)

Life after eruption – IV. Spectroscopy of 13 old novae

C. Tappert,[1⋆] N. Vogt,[1] M. Della Valle,[2] L. Schmidtobreick[3] and A. Ederoclite[4 ⋆†]
[1]*Instituto de Física y Astronomía, Universidad de Valparaíso, Avda. Gran Bretaña 1111, 2360102 Valparaíso, Chile*
[2]*INAF - Osservatorio di Capodimonte, Salita Moiariello 16, 80131 Napoli, Italy*
[3]*European Southern Observatory, Alonso de Cordova 3107, 7630355 Santiago, Chile*
[4]*Centro de Estudios de Física del Cosmos de Aragón, Plaza San Juan 1, Planta 2, Teruel, E44001, Spain*

arXiv:1405.3635v2 [astro-ph.SR] 27 May 2014

Accepted. Received

ABSTRACT
We present data on 13 post-nova systems. This includes the recovery via *UBVR* photometry of the five post-novae X Cir, V2104 Oph, V363 Sgr, V928 Sgr and V1274 Sgr and their spectroscopic confirmation. We provide accurate coordinates and finding charts for those objects. Additional first-time or improved spectroscopic data are presented for V356 Aql, V500 Aql, V604 Aql, V1370 Aql, MT Cen, V693 CrA, V697 Sco and MU Ser. Investigating the behaviour of a few easily accessible parameters yields (limited) information on the accretion state and the system inclination. We predict that X Cir and V697 Sco are likely to reveal their orbital period via time series photometry and that long-term photometric monitoring of V356 Aql, V500 Aql, V1370 Aql and X Cir has a good chance of discovering outburst-like behaviour in these systems.

Key words: novae, cataclysmic variables

1 INTRODUCTION

A classical nova eruption is a thermonuclear runaway on the surface of the primary component of a cataclysmic variable (CV), i.e. an interacting white-dwarf/red-dwarf binary system. This is a bright event: eruption amplitudes range between 8 and 14 mag, and the nova at maximum reaches absolute magnitudes typically from -7 to -9 mag (della Valle & Livio 1995). Novae are thus usually well studied during maximum brightness and for a few weeks or months after. However, once the brightness has declined to a stable 'quiescence' value (which may be fainter, equal to, or brighter than the pre-eruption brightness; Collazzi et al. 2009), detailed investigations become comparatively scarce, mostly because such now need a significant amount of time on large telescopes. Because most Galactic novae are located in the Galactic disc and thus within crowded fields, this has led to the situation that for a large fraction (currently about 50 per cent) of the $\sim$200 novae that were reported before 1980 the position is not known with sufficient accuracy to properly identify the post-nova.

However, the study of post-novae has the potential to provide the answer to several questions concerning the influence of the nova eruption on the CV hosting it (Shara et al. 1986; Johnson et al. 2014) as well as concerning the physical parameters of the CV (magnetic field, masses, mass-transfer rate, chemical composition) affecting the recurrence time of the nova eruption (e.g. Townsley & Bildsten 2005). This is especially true since it is now generally accepted that the nova eruption represents an integral part of CV evolution (e.g. Patterson et al. 2013). However, a comparative study of the overall CV population with that of post-novae even with respect to comparatively easily accessible parameters like the orbital period (Townsley & Bildsten 2005; Tappert et al. 2013b) still lacks statistical significance due to the small sample size of the latter systems. We have thus set out to increase the sample of post-novae by identifying candidates for the post-nova via photometric colour-colour diagrams and confirming them spectroscopically. For more details on the motivation and the methods see Tappert et al. (2012, hereafter Paper I).

In order to minimize the contribution of the ejected material in the visual wavelength range, we usually restrict our study to novae that were reported before 1980. However, in this paper, we additionally include spectroscopic data on a number of systems where the time between maximum brightness and the spectroscopic observations amounts to less than 30 yr. In none of those systems do we find signatures of the ejected material and they thus equally fit our profile, in that they offer an undiluted view on the underlying CV.

2 OBSERVATIONS AND REDUCTION

The $UBVR$ photometric data were taken in 2009, May, using the ESO Faint Object Spectrograph and Camera (EFOSC2; Eckert, Hofstadt, & Melnick 1989) at the ESO-NTT, La Silla, Chile. Typically, a series of $\geqslant$3 frames per filter was obtained.

⋆ E-mail: claus.tappert@uv.cl
† Based on observations with Euorpean Southern Observatory (ESO) telescopes, proposal numbers 083.D-0158(A), 089.D-0505(B), 090-D-0069(B)

Table 1. Log of observations.

Object	RA (2000.0)	Dec. (2000.0)	Date	Filter/Grism	$t_{\rm exp}$ (s)	mag
V356 Aql	19:17:13.71	+01:43:21.7	1993 July 12	B300 (1.5 arcsec)	2400	–
V500 Aql	19:52:28.00	+08:28:46.2	1992 July 8	B300 (2.0 arcsec)	1800	–
V604 Aql	19:02:06.39	−04:26:43.7	2012 June 14	300V (LSS)	2 × 900	18.8R
V1370 Aql	19:23:21.10	+02:29:26.1	1993 July 12	B300 (1.5 arcsec)	3000	–
MT Cen	11:44:00.24	−60:33:35.7	2013 January 12	300V (LSS)	2 × 900	19.5R
X Cir	14:42:41.46	−65:11:18.7	2009 May 20	$U/B/V/R$	1800/900/300/180	19.3V
			2013 March 13	300V (MOS)	2× 888	18.5R
			2013 March 14	300V (MOS)	888	18.7R
V693 CrA	18:41:58.02	−37:31:14.5	1993 July 11	B300 (2.0 arcsec)	3600	–
V2104 Oph	18:03:24.99	+11:47:57.1	2009 May 22	$U/B/V/R$	1800/900/300/180	20.9V
			2012 July 14	300V (LSS)	2× 2700	20.4R
V363 Sgr	19:11:18.90	−29:50:37.8	2009 May 21+22	$U/B/V/R$	3600/900/300/240	19.0V
			2012 April 29	300V (MOS)	2640	19.2R
V928 Sgr	18:18:58.09	−28:06:34.9	2009 May 22	$U/B/V/R$	1800/900/300/180	19.5V
			2012 May 17	300V (MOS)	2 × 2640	19.8R
V1274 Sgr	17:48:56.19	−17:51:51.0	2009 May 20	$U/B/V/R$	1800/900/300/180	19.2V
			2012 June 21	300V (MOS)	2640	18.9R
V697 Sco	17:51:21.91	−37:24:56.9	1992 July 8	B300 (2.0 arcsec)	900	–
MU Ser	17:55:52.78	−14:01:17.1	1993 July 11	B300 (1.5 arcsec)	3600	–

EFOSC2 suffers from a well-known central light concentration that makes proper flat-fielding a difficult and time-consuming process. Since our scientific goal requires only moderately high photometric precision, we refrained from a flat-field correction, and only performed the subtraction of bias frames in the reduction process. Subsequently, the frames were corrected for the individual telescope offsets and averaged using a 3σ clipping algorithm to minimize the effect of bad pixels. Photometric magnitudes for all stars in the fields on both the averaged data and the individual frames (to check for variability) were extracted using the aperture photometry routines in IRAF's DAOPHOT package and the standalone DAOMATCH and DAOMASTER routines (Stetson 1992). These magnitudes were calibrated using observations of standard stars (Landolt 1983, 1992).

The spectroscopic data consist of two sets. The first one was taken on two runs in 1992 and 1993 July, with EFOSC1 mounted on the ESO 3.6 m telescope in La Silla, Chile. The B300 grating was used with a 1.5 arcsec and a 2.0 arcsec slit, resulting in a spectral resolution of ∼15 and ∼20 Å, respectively, over a useful wavelength range of ∼3800–6900 Å. The efficiency curve of B300 peaks in the blue at about 4500 Å. At that time the EFOSC set-up included a Tektronix 512×512 pixel CCD (#26) with a red efficiency curve peaking at ∼6900 Å, resulting in an approximately uniform efficiency over the whole wavelength range. Data reduction was performed with ESO-MIDAS (Warmels 1992) and consisted of bias reduction and flat-field correction. The wavelength calibration that has been performed using a Helium-Argon lamp deviates somewhat blueward of 4100 Å. The spectral energy distribution (SED) was corrected for the response function of the instrument and a formal correction for the atmospheric extinction was performed, but since the data were taken during non-photometric conditions no flux calibration was applied. For a few systems, we find a number of weak and narrow emission lines that we attribute to the extraction process suffering from an imperfect subtraction of the night sky, leaving residuals in the 5000–6000 Å range, especially concerning the [O I] λ5577.338 line.

The second set of spectroscopic observations was performed in service mode at the ESO-VLT using the FOcal Reducer/low dispersion Spectrograph (FORS2; Appenzeller et al. 1998) with grism 300V and a 1.0 arcsec slit. Depending on the number of original candidates in the field, the instrument was operated either in long-slit (LSS) or in multi-object (MOS) mode. Reduction of the data consisted of subtraction of an averaged bias frame and division by a flat field that was previously normalized by fitting a cubic spline of high order to the response function. After optimal extraction (Horne 1986) with IRAF's APALL routine, the spectra were wavelength calibrated using the spectra of comparison lamps. The typical wavelength range is ∼4100–9000 Å at a spectral resolution of ∼11 Å, measured as the full width at half-maximum (FWHM) of the calibration lines. Finally, the data were flux calibrated using observations of spectrophotometric standard stars. Because the data were taken in service mode, the red CCD mosaic (two 2k×4k MIT CCDs) had to be used for the observations. As a consequence of its low efficiency, blueward of ∼4400, Å the SED in that part is not reliable. Other than for the EFOSC data, the acquisition frames (taken in the R passband) were available for the FORS observations. This allowed for a photometric analysis and thus the extraction of a differential R magnitude that was calculated with respect to a number of comparison stars. The apparent R magnitude was subsequently derived with respect to previous photometric data.

Table 1 summarizes the details of the observations sorted in the order of the variable designation. The second and third column contain the coordinates. For the novae with photometric observations (this includes those with acquisition frames) they were determined performing astrometry with Starlink's GAIA[1] tool (version 4.4.3) using the US Naval Observatory CCD Astrograph Catalog (UCAC) version 3 (Zacharias et al. 2010) and 4 (Zacharias et al. 2013). The typical rms resulted to $\leqslant$0.24 arcsec. Coordinates for the other systems were taken from the Downes et al. (2005) or Saito et al. (2013) catalogues. Column 4 states the date of the observations corresponding to the start of the night in local time. Columns 5 and 6 give the instrument configuration, i.e. the filter and grism used, and the corresponding total exposure times,

[1] `http://astro.dur.ac.uk/~pdraper/gaia/gaia.html`

Table 3. Results of the $UBVR$ photometry.

Object	V	$U-B$	$B-V$	$V-R$
X Cir	19.29(12)	−0.45(02)	0.48(03)	0.45(04)
V2104 Oph	20.94(08)	−0.57(03)	0.50(02)	0.41(03)
V363 Sgr	19.02(14)	−0.95(01)	0.16(01)	0.02(01)
V928 Sgr	19.51(08)	−0.55(01)	0.37(01)	0.22(02)
V1274 Sgr	19.15(11)	−0.70(03)	0.42(03)	0.23(02)

respectively. Finally, where available, the last columns states the brightness at the time of the observations with the letter at the end identifying the corresponding passband.

3 RESULTS

In Figs. 1 and 2 we present the spectra taken with the ESO 3.6 m telescope and at the VLT, respectively. For systems with more than one spectrum, the combined data are shown. Equivalent widths (W_λ) of principal emission lines in these spectra are collected in Table 2 [2]. The corresponding errors were estimated with a Monte Carlo simulation by adding random noise to the data and repeating the measurement a thousand times. Fig. 3 presents the $U-B/V-R$ colour-colour diagrams for the five systems with respective data, and Table 3 details the corresponding values.

For the analysis of the spectra, we have used the values for interstellar extinction $E(B–V)$ from Schlafly & Finkbeiner (2011) using NASA's Infrared Science Archive web pages. The values are listed in Table 4 and represent the average extinction within a 2×2 degree field. They were used to deredden the spectra employing the corresponding IRAF task, which is based on the relations derived by Cardelli, Clayton, & Mathis (1989). A standard value for the ratio of the total to the selective extinction $R(V) = A(V)/E(B–V) = 3.1$ was used. The dereddened spectra were fitted with a power law $F \propto \lambda^{-\alpha}$, restricting the continuum to wavelengths 5000–7200 Å and masking strong emission and absorption lines.

We furthermore folded the flux calibrated (VLT) spectra with Bessell (1990) passbands to obtain spectrophotometric magnitudes. A comparison for those systems with information on photometric magnitudes suggests slit losses $\leqslant$0.5 mag.

3.1 V356 Aquilae = Nova Aql 1936

This relatively slow nova was discovered by N. Tamm, Kvistaberg Observatory, Denmark, on 1936, September 18 as an object of eighth magnitude (Strömgren 1936; Duerbeck 1987). McLaughlin (1955) describes the eruption light curve as a fast rise from July 17 to 19 followed by a more gradual rise and irregular fluctuations over several months. The recorded maximum value was 7.1 mag on October 3, although the primary maximum is suspected to have occurred during an unobserved period between July 31 and August 10. Robinson (1975) lists the pre-eruption magnitude to 16.5 mag. However, Szkody (1994) finds the post-nova at V = 18.3 mag in 1988, and Ringwald, Naylor, & Mukai (1996) report V = 17.9 mag in 1991. Woudt, Warner, & Pretorius (2004) present high-speed photometry revealing flare-like outburst activity at time-scales of about 50 min, but no coherent periodicities. Duerbeck & Seitter (1987) describe the spectrum of V356 Aql as a blue continuum with strong Hα and weaker Hβ emission, as well as with a strong Bowen/He II emission component. Ringwald et al. (1996) present a spectrum with medium strong Hα (W_λ = 15 Å). They also detect He I λ6678, while the blue part has too low S/N to reveal any details.

Our spectrum taken at the ESO 3.6 m telescope shows emission lines over a red continuum (Fig. 1). The latter differs strongly

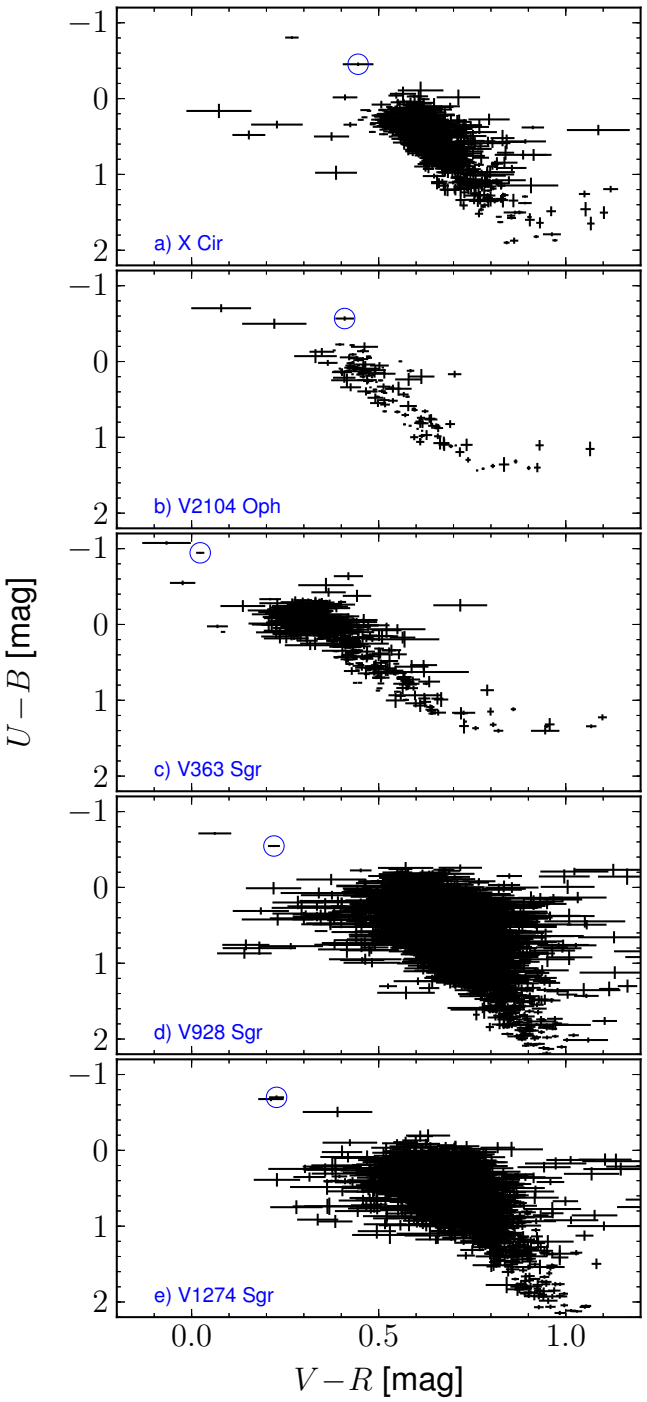

Figure 3. Colour-colour diagrams. The confirmed post-novae are marked with a circle.

[2] For convenience, we use positive values for W_λ. This is unambiguous since we exclusively refer to emission lines.

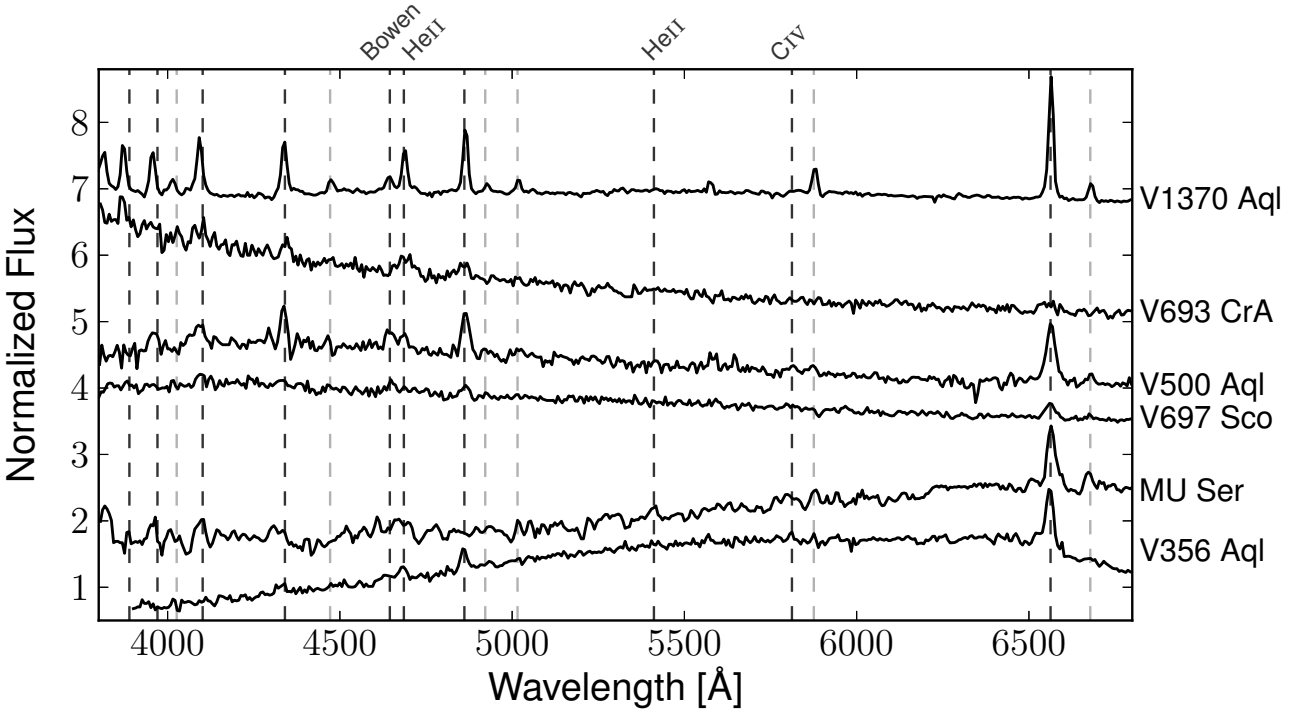

Figure 1. EFOSC spectra. Unlabelled black vertical dashed lines mark the positions of Balmer emission, grey lines indicate the He I series.

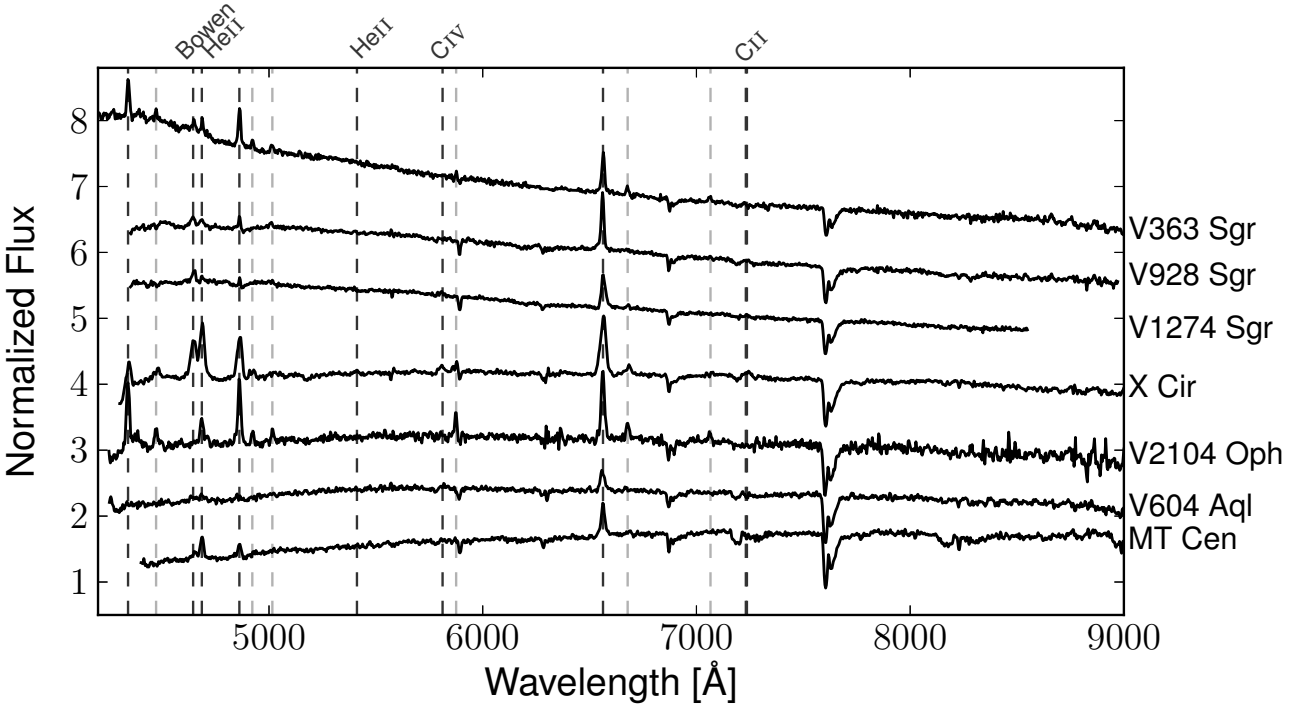

Figure 2. FORS2 spectra. Unlabelled black vertical dashed lines mark the positions of Balmer emission, grey lines indicate the He I series.

from the description of Duerbeck & Seitter (1987) and the spectrum published by Ringwald et al. (1996). The spectrum was taken at a fairly high air mass $M(z)$ = 2.1 and it is thus possible that the continuum slope is affected by a non-parallactic position angle of the slit. With respect to the emission lines, our data better fits that of Duerbeck & Seitter (1987), with the Hα emission being considerably stronger than in the Ringwald et al. (1996) data (Table 2). In the blue part of the spectrum we furthermore identify Hβ, the adjacent He I λ4922 line, a medium strong Bowen/He II blend and Hγ. Higher Balmer lines fall victim to the strong Balmer decrement and the low S/N. Apart from the usual residuals of the night sky lines in the 5000–6000 Å range, we also find a couple of emission spikes that reasonably coincides with the positions of C IV λ5812 and He I λ5876. Another, double, spike is close to He II λ5412. However,

Table 2. Equivalent widths in angstroms of the principal emission lines. A blank field means that the line was not included in the spectral range, a '$-$' means that the line was not detected. Values in square brackets refer to emission cores within absorption troughs.

Object	Balmer			He I						Bowen/He II	He II	C IV
	4340	4861	6563	4472	4922	5016	5876[a]	6678	7065	4645/4686[b]	5412	5812
V356 Aql	6(1)	7(1)	29(2)	–	2(2)	–	–	2(2)		12(3)	–	–
V500 Aql	9(2)	18(2)	41(3)	1(1)	6(1)	5(1)	4(2)	4(2)		11(1)	–	4(2)
V604 Aql	–	1.5(3)	7.9(5)	–	–	–	2.4(3)	0.6(2)	–	5.2(6)	–	–
V1370 Aql	20(1)	20(1)	39.1(5)	4.4(5)	2.8(9)	3.5(6)	7.1(5)	5.4(6)		23(1)	–	–
MT Cen		4.9(9)	10.3(3)	–	–	–	–	1.0(3)	–	12.8(5)	–	–
X Cir	11(2)	17.5(5)	28.1(4)	3.5(5)	3(1)	1.7(5)	2.5(5)	3.1(6)	1.0(1)	43.5(8)	0.8(3)	2.6(3)
V693 CrA	5(1)	9(2)	11(3)	1.7(9)	–	–	–	–		12(2)	–	–
V2104 Oph	18(1)	18(1)	18.7(7)	6(1)	2.8(4)	2.4(6)	4.9(5)	3.9(3)	2.0(4)	9.1(7)[c]	–	–
V363 Sgr	4.1(2)	5.2(3)	11.5(5)	0.9(2)	0.8(2)	0.8(2)	0.9(1)	2(0.5)	2(0.5)	3(0.5)	–	–
V928 Sgr		[1.8(1)]	14.3(4)	–	–	1.2(2)	–	0.6(5)	–	4.5(4)	–	–
V1274 Sgr		[0.4(1)]	11.5(4)	–	–	0.7(2)	–	0.9(1)	–	4.4(4)	–	0.9(2)
V697 Sco	2(2)	[4(2)]	9.7(7)	–	0.9(7)	–	–	2.1(8)		2.7(8)[d]	–	–
MU Ser	18(2)	–	23(2)	–	–	–	–	4(1)		14(4)	5(2)	7(2)

[a] this line is mostly distorted by the adjacent Na I absorption.
[b] the two components are not resolved.
[c] He II 4686 only; [d] Bowen blend only

since in appearance (FWHM) and strength they are more similar to the night sky residuals than to the other intrinsic emission lines, we do not consider those spikes as sufficient evidence for the presence of those lines.

3.2 V500 Aquilae (Nova Aql 1943)

According to Duerbeck (1987), this object was detected by Hoffmeister on plates of the Sonneberg Observatory, Germany. The recorded maximum light of 6.55 mag was reached on 1943 May 2, although the real maximum can be suspected to have occurred sometime before that. Cohen (1985) detected a small shell around the ex-nova, with a diameter of the order of 2 arcsec, and an expansion velocity of 1380 km s^{-1}. Szkody (1994) finds the post-nova at V = 19.3 mag. Time-resolved photometry by Haefner (1999) during two nights in August 1994 revealed that V500 Aql is an eclipsing binary with a period of 3.5 h and an eclipse depth of the order of 0.5 mag, with superimposed flickering. The only spectroscopic data to date come from the radial velocity study by Haefner & Fiedler (2007) that has a high spectral resolution of 1.2 Å but covers only a limited wavelength range of 4000-5000 Å. The spectra show a weak Balmer series (Hβ to Hδ) and a moderately strong Bowen/He II blend. Complex changes at different orbital phases can be recognized, especially in the Balmer line profiles. In spite of being an eclipsing system, the emission lines in almost all phase bins are single peaked. This is similar to the behaviour of the SW Sex-type stars (Thorstensen et al. 1991) which represent the dominant population in the 3–4 h orbital period range (Rodríguez-Gil et al. 2007). The fact that the period of V500 Aql lies within this regime thus fits well into this picture.

Our spectrum shows a blue continuum and unusually strong emission lines for an old nova (Fig. 1). In contrast to the Haefner & Fiedler (2007) spectra, we can clearly identify the He I $\lambda\lambda$4471 and 4922 lines, which perhaps are hidden in the lower S/N of their data. Like for V356 Aql (Section 3.1), we find a few emission spikes in the 5000–6000 Å range that we do not believe to be intrinsic emission lines due to their smaller FWHM. However, the components corresponding to the positions of C IV λ5812 and He I λ5876 look sufficiently convincing. Their presence is also in agreement with the general appearance of the spectrum, namely that a large number of He I lines can be identified, and that the Bowen C/N component is at least as strong as the adjacent He II λ4686 line.

3.3 V604 Aquilae (Nova Aql 1905)

This relatively fast nova was discovered on Harvard plates by W. Feming on 1905, August 31, but additional plates, taken a few weeks earlier, place the photographic maximum brightness of 8.2 mag to mid-August 1905, fading rapidly afterwards. Duerbeck (1987) gives the references on the early literature. Photometric $BVRJK$ data of the object were obtained by Szkody (1994), determining the minimum light to $V \sim 19.6$ mag. A 3.5 h CCD light curve was published by Haefner (2004). It exhibits erratic short-term variations with amplitudes up to about 0.25 mag, but also a longer lasting structure that bears some resemblance to an orbital hump.

The spectrum of the star marked in Downes et al. (2005) shows weak and narrow emission lines (Fig. 2). The continuum peaks at $\sim$5600 Å. However, the extinction amounts to $E(B-V)$ $\sim$0.7 mag, and after dereddening the spectrum with this value, we find a slope that corresponds to a power-law index α $\sim$2.1 which is a rather typical value for high $\dot{M}$ post-novae (Paper I). The slope flattens slightly towards the blue part of the spectrum. For the potentially magnetic nova V630 Sgr such has been interpreted as a signature for a disrupted inner accretion disc (Schmidtobreick et al. 2005), but in V604 Aql the difference in slopes is much less clear.

Comparison of the acquisition frame with the UCAC4 catalogue indicates an R-band brightness $\sim$18.8 mag. Folding the spectrum with Bessell passbands yields V = 19.8 mag and R = 19.3 mag. Taking into account a probable slit loss $\leqslant$0.5 mag as observed for the other FORS2 spectra, we find that these results agree well with each other. Those values are not significantly different from those measured by Szkody (1994) in 1988 April (V = 19.6 and R = 19.1 mag) especially considering the amplitude of the variability observed by Haefner (2004).

3.4 V1370 Aquilae (Nova Aql 1982)

As reported in Kosai et al. (1982), the nova was discovered by M. Honda in Japan, 1982 January 27. An analysis of the eruption light curve by Rosino, Iijima, & Ortolani (1983) suggests that maximum light was reached a few days earlier and up to two magnitudes brighter than the recorded value of 6.5 mag. They classify the object as a fast nova with t_3 ∼10 d. For the corresponding literature during the first years after outburst maximum see Duerbeck (1987) and Snijders et al. (1987). A comprehensive analysis on the eruption of V1370 Aql can be found in Smits (1991), combining several aspects including the light curve, the high expansion velocity, as well the spectral development in the UV, IR and optical range, and the elemental abundances in the ejected shell. Strope, Schaefer, & Henden (2010) file the nova into the 'D' class, meaning that there was a dip in the eruption light curve, indicating the formation of dust. Szkody (1994) finds the post-nova at V = 18.0 mag seven years after maximum brightness, while Ringwald et al. (1996) lists V = 18.5 mag two years later. The latter authors furthermore present a spectrum that shows very strong Balmer emission lines (W_λ = 43 Å for Hα) and the presence of the He I series, but – only nine years after the eruption – already no sign of nebular emission.

Our spectrum in Fig. 1 was taken one year after the one presented in Ringwald et al. (1996). It is quite unusual for an old nova, in that it shows an extremely hydrogen and He I rich emission line forest. While in other old novae, the higher Balmer lines >Hδ tend to be hidden in the absorption lines of an optically thick disc, the Balmer series in V1370 Aql can be followed up to the limit of our blue spectral range, the last line that can be clearly identified being H11 λ3771. The Balmer decrement in general is also comparatively flat, indicating an optically thin disc. The only exception represents Hα which has about twice the strength of Hβ, suggesting the presence of an additional Hα emitter. The He I series is remarkably well pronounced. Even weak lines like λ4026, λ4388 (as an emission hump on the red wing of Hγ) and λ5048 are clearly discernable. Overall, V1370 Aql has more the appearance of a (comparatively) low mass-transfer CV than of an old nova, with the exception of the presence of a quite prominent Bowen/He II component and of the absence of other low $\dot{M}$ indicators like Ca II and Fe I emission (see e.g. the spectrum of GZ Cnc which otherwise has similar characteristics as V1370 Aql; Tappert & Bianchini 2003). The signatures of an optically thin disc are the more remarkable as the emission lines are quite narrow, indicating that the system inclination is low, and thus that a large fraction of the disc should be able to contribute to the radiation from the system. An optically thin and thus intrinsically faint disc would also support above idea that the system at maximum was considerably brighter than the recorded 6.5 mag, since the resulting eruption amplitude of 11.8 mag (Table 4) appears too low for such a system and thus should be regarded as a lower limit.

3.5 MT Centauri (Nova Cen 1931)

The spectroscopic confirmation of this nova was already reported in Paper I and we refer the reader to that publication for a summary on the available data. In the meantime, the object has also been identified in the VISTA Variables in the Vía Láctea Survey (VVV), with Saito et al. (2013) providing infrared magnitudes. The spectrum in Paper I suffered from very low S/N and thus revealed very little detail on the emission lines. The FORS spectrum presented in Fig. 2 is of much higher quality and allows for the additional identification of the He I λ6678 emission line. We furthermore note that the Bowen/He II blend is clearly dominated by the helium emission.

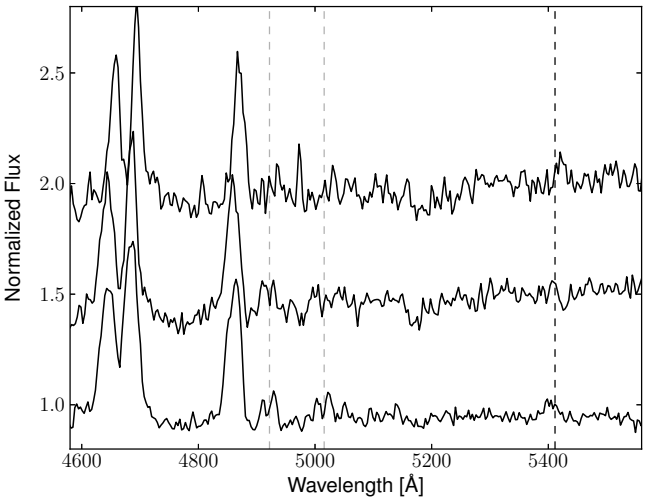

Figure 4. Close-up on the blue part of the three spectra of X Cir. He I positions are marked by dashed grey lines, the position of He II 5412 is indicated by the black dashed line.

As in Paper I, the spectrum shows a red slope that is entirely due to interstellar reddening. After the corresponding correction, the SED is that of a high $\dot{M}$ system with a power-law index of α = 3.44(1). This is somewhat less than what was determined for the Paper I spectrum (α = 4.45(7)). However, the major portion of this difference is due to the use of the revised extinction value from Schlafly & Finkbeiner (2011) in this paper with respect to Schlegel, Finkbeiner, & Davis (1998) that was used in Paper I, i.e. $E(B-V)$ = 1.38(2) instead of 1.61(2). Applying the old value for the correction of the new spectrum yields α = 4.12(1).

Even with the new extinction value, the dereddened slope is much steeper than for the other systems. However, other indicators of high $\dot{M}$, like the weakness of the Balmer emission, point to a somewhat lower $\dot{M}$ than e.g. for V928 Sgr and V1274 Sgr (Sections 3.10 and 3.11, respectively), both with a significantly lower slope (Table 4). It appears thus reasonable to assume that only part of the dust that causes the high extinction in this region lies in the line of sight to MT Cen, and that applying the full extinction value overcorrects the reddening of its SED.

3.6 X Circinis (Nova Cir 1926)

The nova was discovered spectroscopically on an objective prism plate taken at La Paz, Bolivia, 1927, May 21, by Becker (1929). At the time of discovery, it had a photographic brightness of about 11.0 mag. A search on archive plates by Cannon (1930) revealed that the maximum brightness of 6.5 mag was reached on 1926 September 3. Duerbeck (1987) lists it thus as a slow nova with t_3 = 170 d. Woudt & Warner (2002) report a candidate for the post-nova, based on flickering activity. However, a spectrum taken by Mason & Howell (2003) of this object presents only absorption lines and a comparatively red continuum peaking at ∼6000 Å, making this an unlikely candidate for the post-nova.

Our $UBVR$ photometry of X Cir yields a number of potential candidates (Fig. 3, top). While the object that turned out to be the nova is certainly one of the two most interesting ones colourwise, we had it nevertheless listed as one of the minor candidates, because first, with ∼1.3 arcmin it lies at quite a distance from the

reported coordinates, and secondly, the point spread function (PSF) on all photometric frames and also in the 2-D spectrum appears slightly elongated at an angle of roughly 50° as counted from north to east. Unfortunately, the PSFs of the images in different filters vary considerably probably due to insufficient focus correction, and thus do not allow for an analysis of the extended object in this respect. On the other hand, the 2-D spectrum suggests that the emission lines are confined to the eastern part of the PSF. Our preliminary conclusion is that this is a close visual binary with a separation $<$0.6 arcsec, with the nova being the north-eastern component.

The spectrum of X Cir is quite remarkable (Fig. 2). For a nova, it presents comparatively strong hydrogen emission lines that allows even for the detection of the blue end of the Paschen series (from Pa13 λ8665 on). The contribution of He II is considerable, as is evident from the presence of the λ5412 line. We furthermore detect carbon in the form of the C IV λ5812 line and the C II $\lambda\lambda$7231/7236 doublet. This combination makes for a particularly strong Bowen/He II blend, similar to what is observed in the old nova V840 Oph (Schmidtobreick et al. 2003).

In Fig. 4 we have plotted a close-up on the blue part of the three individual spectra. The first spectrum taken (on HJD 245 6365.70523) is shown at the bottom, the middle spectrum was obtained 3.0 h later (HJD 245 6365.83078), and the top spectrum was taken 27.6 h after the first one (HJD 245 6366.85626). The spectra have been normalized by dividing through the mean value of the $\lambda\lambda$4500–5600 Å range and displaced vertically. We note that the He I lines are distinctively double peaked with the central valley in some lines reaching the continuum level. All other lines are single peaked. In the case of the Balmer series, however, it can be clearly seen that there is an additional emission component superposed on the (potentially) double-peaked profile. The same component is also present in the He I lines. Note how in the bottom spectrum the red peak is broader than the blue one, while the opposite can be observed in the middle spectrum. The asymmetry in the Hβ line behaves in the same manner. In old novae, an irradiated secondary star is a likely source of such additional emission, but with the limited present data other possibilities can of course not be excluded. The He II and carbon lines, on the other hand, while single-peaked, do not present any discernable additional contribution but a broad single-peaked profile.

We furthermore observe that the He II λ5412 line is well above continuum level in the bottom spectrum, below an unambiguous detection in the middle spectrum and again clearly present in the top spectrum. Because the individual exposure times amount to only 15 min, this could represent an orbital effect. This becomes even more likely when one considers that the double-peaked He I lines let suspect a comparatively high system inclination. Comparing the relative brightness of the continuum between $\lambda\lambda$5000 and 5400 Å, we find that the middle and top spectra are fainter than the first by $\sim$0.4 and $\sim$0.7 mag, respectively. From the acquisition frames, we compute the brightness in the R band to 18.47(02) mag just before the first spectrum was taken and to 18.71(02) mag just before the third spectrum. Such differences are not unusual for CVs seen at high inclination, and the brightness is thus also consistent with the photometry from 2009 (R = 18.84(12) mag; see Table 3).

3.7 V693 Coronae Austrinae (Nova CrA 1981)

As reported by Kozai et al. (1981) this fast nova was discovered by M. Honda in Japan, 1981 April 2 at a visual brightness of 7.0, while it was invisible one day earlier. Williams et al. (1985) observed its eruption over several months with the International Ultraviolet Explorer (IUE) satellite and on the basis of the derived elemental abundances conclude that the nova contains a massive ONeMg white dwarf. A re-analysis of archival IUE data by Vanlandingham, Starrfield, & Shore (1997) agrees with this result as does the recent work by Downen et al. (2013), who use actual thermonuclear eruption models in combination with elemental abundance determinations during the eruption to determine the white dwarf mass to $\leqslant$1.3 M$\odot$. Schmidtobreick et al. (2002) report V = 21.0 mag for the post-nova.

Due to the faintness of the object, our spectrum taken at the ESO 3.6 m telescope is of limited quality (Fig. 1). It shows a steep blue continuum with rather weak Balmer lines. Of the He I series, only the line at 4472 Å can be reasonably well identified. The emission lines are very broad, which could indicate a high inclination, or, since the FWHMs for different lines span quite a range (26 Å for Hγ, 32 Å for Hβ, 43 Å for Hα), possibly contamination from the shell material. Overall, this is certainly a high $\dot{M}$ CV.

3.8 V2104 Ophiuchi (Nova Oph 1976)

The nova was discovered on 1976 September 23 at a visual brightness of 8.8 mag (Osawa & Kuwano 1976). In spite of being a comparatively young nova, the post-eruption coverage is poor. Huth (1976) measures a pre-maximum photographic brightness of 9.3 mag for 1976 September 22, and a fading to 12.4 mag for October 21. This yields an upper limit for t_3 of 28 d. Robertson et al. (2000) report a candidate for the post-nova with B = 21.0 mag that is Hα bright according to a private communication by Downes. A search for a shell by Downes & Duerbeck (2000) remained unsuccessful, but they report the same object at V = 20.5.

The colour-colour diagram (Fig. 3) indicates a couple of blue, but very faint, objects, while the Robertson et al. (2000) candidate is comparatively red and about half a magnitude fainter than previously reported (Table 3). Nevertheless, its spectrum shows the typical emission lines that confirm the nova (Fig. 2). Like in X Cir (Section 3.6), the Balmer and He I lines are comparatively strong, but in the case of V2104 Oph they are much more narrow. The typical FWHM of a line amounts to $\sim$16 Å and lies thus only slightly above the spectral resolution. We furthermore note that there is no detectable Bowen component, but that He II λ4686 is clearly present, if not particularly strong. The continuum is comparatively flat, which appears to be intrinsic since there is little interstellar extinction in this region of the sky (Table 4), and does not show any detectable contribution from the secondary star.

The strengths of the lines and the flat continuum suggest that V2104 Oph has comparatively low $\dot{M}$. We also note that the (dereddened) spectral slope cannot be fitted by a single power law, but shows two vastly different slopes blue- and redward of $\sim$5670 Å, with both individual power indices being well below a steady-state disc (Table 4 and Section 4). The narrowness of the emission lines translates to a narrow range of sampled velocities. Since we do not see any correlation of the FWHM with the line species or degree of ionization, this indicates that the object is seen at a low inclination. This makes it unlikely that the brightness difference of our data with respect to the measurements by Robertson et al. (2000) and Downes & Duerbeck (2000) is due to orbital variability.

3.9 V363 Sagittarii (Nova Sgr 1927)

An objective prism spectrum taken on 1927 September 30 showed emission lines in an object with a brightness of $\sim$11 mag (Becker

1930). An archival search by Walton (1930) confirmed the suspicion of a nova event and revealed that the photographic maximum brightness of 8.8 mag had already been reached on August 3 and perhaps even somewhat earlier (because of a lack of observations from July 1 to August 2). Duerbeck (1987) gives two potential candidates for the post-nova.

However, V363 Sgr was recovered via its position in the colour-colour diagram (Fig. 3) roughly 40 arcsec outside the area marked in Downes et al. (2005) and thus corresponding to neither of the two Duerbeck (1987) candidates. The spectrum (Fig. 2) shows a steep blue continuum and weak narrow emission lines. Apart from the Balmer and He I series, we can identify the Bowen blend and He II λ4686. Contrary to the other systems in this paper, these two are almost fully separated in V363 Sgr. The spectral appearance suggests that V363 Sgr is seen at a similar low inclination as V2104 Oph, but accretes at significantly higher rates.

3.10 V928 Sagittarii (Nova Sgr 1947)

Burwell (1974) reported this slow nova as an Hα bright star of nineth magnitude based on an object prism plate taken on 1947 May 16. Bertaud (1947) measures a visual brightness of ∼8.9 mag on May 24. Campos & Sanchez (1987) provide finding charts of variable stars in the constellation of Sagittarius, one of which (their object 'L') Morel (1987) identifies with V928 Sgr. He provides revised coordinates that match the third possible position given by Duerbeck (1987).

The colour-colour diagram of the field indicates a couple of blue objects, with the nova turning out to be the brighter of the two roughly 3 arcsec west and 29 arcsec south of above position. The spectrum in Fig. 2 shows a comparatively steep blue continuum that after dereddening gains a slope that within the errors is identical to that of V363 Sgr (Table 4). However, while that system shows a rich emission line spectrum, very few lines can be identified in V928 Sgr. This is in part due to the low blue efficiency of the CCD affecting the spectrum already blueward of 4400 Å so that of the Balmer series only Hα and Hβ lie within the useful spectral range. There, we can observe a very strong Balmer decrement, with the Hβ emission lying partly within an absorption trough. We furthermore identify the Bowen/He II blend. Other than in most other systems where the He II line is the stronger of the two (Ringwald et al. 1996), the corresponding equivalent widths in V928 Sgr are W_λ = 1.8 and 1.2 Å for the individual peaks of the Bowen blend and He II, respectively. The He I series is also peculiar, in that the line at 5016 Å is by far the strongest one, with in fact the line at 6678 Å being the only other, barely, discernable He I emission within our spectral range.

3.11 V1274 Sagittarii (Nova Sgr 1954 No.2)

Wild (1954) discovered this nova as a 10.5 mag star on 1954 August 30. Wenzel (1992) identified the nova on Sonneberg patrol plates, and by combining them with previous data found that while the object was at 12 mag on August 2 and 3, five observations over a range of 38 d, from August 26 to October 3, always showed it at roughly 10.4 mag. This would suggest a classification as a slow nova.

There are two blue stars with very similar colours in the field of V1274 Sgr (Fig. 3). The nova is the one that is slightly bluer in $U-B$ and slightly redder in $V-R$. It is also closer to the originally suspected position, being just inside the circle from the Downes et al. (2005) chart. The spectrum of the other object shows a blue continuum with Balmer and (probably interstellar) Na I absorption. With an FWHM ∼25 Å, the Balmer lines appear too narrow for a white dwarf, and thus this is probably an early B star.

The nova shows the appearance of a high $\dot{M}$ system, with few and weak emission lines and Hβ being visible only as a narrow emission core within an absorption trough (Fig. 2). The blue continuum becomes significantly steeper after dereddening due to the high interstellar extinction in this region (Table 4). We furthermore note the presence of the same carbon emission lines as in X Cir (C IV λ5812 and C II $\lambda\lambda$7231/7236) but also that He II is much weaker than in that system. As a consequence, the Bowen component is much stronger than the adjacent He II λ4686 line (W_λ for the individual peaks are 2.9 and 1.3 Å, respectively).

3.12 V697 Scorpii (Nova Sco 1941)

The nova was discovered by Mayall (1946) on Harvard objective prism plates from 1941 March 9 as an object of 10.2 mag. Analysis of the light curve and the spectra suggest that the maximum eruption brightness occurred sometime before that date. Duerbeck (1987) estimates the true maximum brightness to ∼8 mag and classifies it as a very fast nova with t_3 <15 d. Warner & Woudt (2002) obtained high speed photometry during a total of six nights in May and June 2001. They found the ex-nova at brightnesses V = 19.5–20.1 mag, about 3 mag fainter than previously reported. Their light curves are characterized by rather strong variability with amplitudes up to 0.5 mag. A Fourier analysis of these observations reveals two periodicities, simultaneously present. Based on these observations, the authors consider V697 Sco as an intermediate polar with an orbital period $P_{\rm orb}$ = 4.49 h and a spin period of the white dwarf $P_{\rm rot}$ = 3.31 h. Such proximity of $P_{\rm rot}$ and $P_{\rm orb}$ is observed only in a small number of CVs, e.g. also in the system EX Hya (Vogt, Krzeminski, & Sterken 1980), while most other intermediate polars have $P_{\rm rot} \sim 0.1\ P_{\rm orb}$ (Ritter & Kolb 2003, update 7.20, 2013). Saito et al. (2013) give revised coordinates and *JHK* photometry values from the VVV survey.

Our spectrum (Fig. 1) shows a moderately blue continuum with weak emission lines. Unfortunately the low S/N does not reveal much detail. However, we do find that the Hβ emission line is embedded in shallow absorption troughs. This, and the relative strength of the Bowen blend indicates a high $\dot{M}$. We furthermore remark on the apparent absence of He II λ4686 emission. Considering the suspected high $\dot{M}$ and magnetic nature of the system, this comes as somewhat of a surprise. On the other hand, the abovementioned intermediate polar EX Hya inhabits only a very weak He II λ4686 emission line itself (e.g. Williams 1983), and such a weak contribution in V697 Sco might be hidden in the noise. Clearly, further high S/N data are much desirable for this system.

3.13 MU Serpentis (Nova Ser 1983)

This extremely fast nova was discovered by Wakuda (1983) on 1983 February 22 at a brightness of 7.7 mag. Since it was fainter then 11 mag the day before, this value will be close to maximum brightness. Schlegel, Honeycutt, & Kaitchuck (1985) analyse the eruption light curve to find an upper limit for the maximum to ∼7.3 mag and derive t_3 = 5.3(1.6) d. To our knowledge, there are no further data on the post-nova.

In Fig. 1, we present a spectrum that was taken 10 yr after the eruption. It shows a red continuum slope that we largely attribute

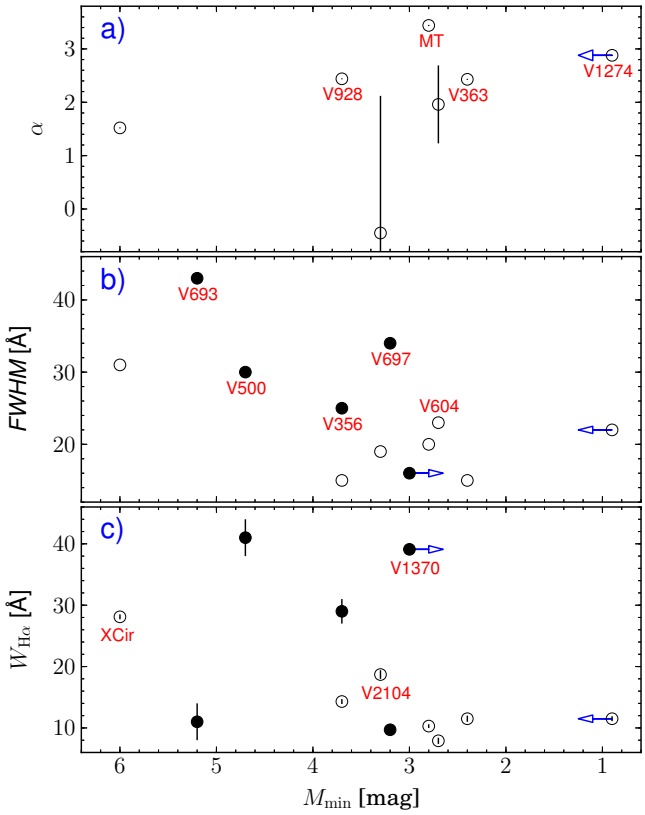

Figure 5. The absolute minimum magnitude $M_{\rm min}$ versus the slope parameter α of the reddening corrected continuum (top), versus the FWHM of the Hα emission line (middle), and versus its equivalent width (bottom). The systems of our sample with spectrophotometric calibration are marked by open circles, those without by solid circles.

to the high extinction in that region (Table 4). The spectrum has fairly low S/N and we have thus smoothed it with a 3 pixel box filter prior to the analysis. We detect moderately strong Hα, Hγ and even higher Balmer lines, but to our astonishment, we do not find any line at the position of Hβ. The higher S/N at the red end of the spectrum also reveals He I λ6678, while the bluer lines of that series are probably hidden in the noise. We furthermore report the likely presence of He II λ5412 and possibly also C IV λ5812. Thus, MU Ser has the appearance of a high $\dot{M}$ post-nova. However, like for V697 Sco (Section 3.12), higher S/N data will be needed to properly analyse the spectroscopic characteristics.

4 DISCUSSION

In Table 4, we have selected several properties of the novae. Column 2 gives the recorded maximum brightness as taken from the references specified in the corresponding chapters above. Column 3 gives the brightness of the post-nova, either from our own photometric data, or as the average of the data found in the literature. Δt in column 4 represents the time from the eruption to the date of the spectroscopic data, while t_3 gives the time of decline to 3 mag below maximum brightness as listed in Duerbeck (1987) or Strope et al. (2010). The time of decline to 2 mag in column 6 was determined from the eruption light curves, but for V928 Sgr and V1274 Sgr, where t_2 was calculated from t_3 using the equations given in Capaccioli et al. (1990). Details on the parameters in columns 7 and 8 are given in the introduction to Section 3. Column 9 contains the FWHM of the Hα emission line that can serve as an indicator for the system inclination. In contrast to Paper I, we have not used Hβ here, because in a few of the here present systems this line is found partly in absorption. Since both decline time and the (absolute) maximum brightness M of the nova eruption can be assumed to mostly depend on the mass of the white dwarf (Livio 1992), it is possible to find a relation between those two parameters, the famous maximum-magnitude versus rate-of-decline relation. We have used the corresponding equation derived by della Valle & Livio (1995) to calculate the absolute maximum magnitudes $M_{\rm max}$ in column 10. Adding the eruption amplitude Δm finally yields the absolute minimum magnitudes $M_{\rm min}$ in column 11. We do not attempt to derive distances because the proper correction for the interstellar absorption is unknown. The example of MT Cen (Section 3.5) shows that this needs a careful analysis of interstellar absorption lines and thus high-resolution and high-S/N data.

While a proper study of possible relations between the parameters in Table 4 needs a sample of more significant size than currently available, in Fig. 5 we use them as a check on the consistency of our results reported in Section 3. For example, the exponent α of the power law fitted to the continuum slope should reflect the brightness of the accretion disc (if present), and should thus be related to $M_{\rm min}$ because the brightness in the visual range of a CV is dominated by the luminosity of the accretion disc. The top plot of Fig. 5 indeed shows a tendency that brighter systems have a steeper continuum slope. The two systems with large error bars for α are V604 Aql and V2104 Oph, where two different slopes were needed to fit the continuum (Sections 3.3 and 3.8). For the plot, we have used the average value, with the error bars corresponding to the difference between the values. The arrows in the plot mark systems with upper or lower limits in the parameters used to derive $M_{\rm min}$.

In the middle plot of Fig. 5, we test as a second example the behaviour of the FWHM of the Hα emission line as a function of $M_{\rm min}$. The faintness of a post-nova can either be due to the absence of an accretion disc (i.e. in polars), due to the disc being intrinsically faint indicating a low $\dot{M}$, or due the system being seen at high inclination (or, of course, a combination of those). Because a high system inclination i yields a larger range of projected values $v \sin i$ for both the velocities in the disc and the velocities of the stellar components, the FWHM of the emission lines can be used as an indicator for i. In the corresponding plot, we find that it is likely that the faintness of V693 CrA (which has the highest FWHM) is at least in part due to a high i and that it does not reflect a low $\dot{M}$. We will come back to this in the next paragraph. The object with the faintest $M_{\rm min}$, X Cir, on the other hand, is also seen at high inclination. However, the difference in brightness to the other systems appears too large to be an exclusive effect of a high i and it is thus likely that the system additionally inhabits an intrinsically faint disc. Last, not least, V697 Sco has comparatively broad emission lines, but still is placed among the brighter systems in our sample. We can thus conclude that this post-nova still drives a very high $\dot{M}$.

Finally, the equivalent width W_λ of the emission lines has been proven a fairly good indicator for $\dot{M}$ in disc systems, with low-$\dot{M}$ presenting strong emission lines and high-$\dot{M}$ correspondingly weak ones (Patterson 1984). In the bottom plot of Fig. 5, we show the respective values of the Hα emission (Table 2). We find that most of the systems in our samples appear to be high $\dot{M}$ systems with weak emission lines ($W_\lambda < 20$ Å). Only four post-novae (X Cir, V500 Aql, V356 Aql and V1370 Aql) can be suspected to have comparatively low $\dot{M}$.

Table 4. Selected parameters of the post-novae. See Section 4 for details.

Object	$m_{\max}$ [a] (mag)	$m_{\min}$ (mag)	Δm (mag)	Δt (yr)	t_3 (d)	t_2 (d)	$E(B-V)$ (mag)	α	FWHM(Hα) (Å)	$M_{\max}$ (mag)	$M_{\min}$ (mag)
V356 Aql	7.1p	18.0V	10.9	57	140	36	0.40(2)	–	25	-7.2	3.7
V500 Aql	6.6p	19.3V	12.7	49	42	19	0.147(1)	–	30	-8.0	4.7
V604 Aql	8.2p	19.6V	11.4	107	25	8	0.69(1)	1.62(4) / 2.29(2) [b]	23	-8.7	2.7
V1370 Aql	$<$6.5v	18.3V	$>$11.8	11	$\sim$10	7	0.41(2)	–	16	-8.8	$<$3.0
MT Cen	8.4p	19.8V	11.4	82	$\sim$10	11	1.38(2)	3.44(1)	20	-8.6	2.8
X Cir	6.5p	19.3V	12.8	87	170	160	0.42(2)	1.52(1)	31	-6.8	6.0
V693 CrA	7.0v	21.0V	14.0	12	18	6	0.0985(6)	–	43	-8.8	5.2
V2104 Oph	8.8v	20.9V	12.1	36	$<$29	6	0.15(1)	$-$1.69(5) / 0.80(3) [b]	19	-8.8	3.3
V363 Sgr	8.8p	19.0V	10.2	85	64	22	0.103(4)	2.43(1)	15	-7.8	2.4
V928 Sgr	8.9p	19.5V	10.6	65	150	88	0.39(1)	2.440(9)	15	-6.9	3.7
V1274 Sgr	10.4p	19.2V	8.8	58	$\gg$38	$\gg$20	0.52(5)	2.88(1)	22	>-7.9	$>$0.9
V697 Sco	$\sim$8p	20.0V	$\sim$12	51	$<$15	8	0.43(2)	–	34	-8.8	3.2
MU Ser	7.7v	–	–	10	5	2.5	0.77(4)	–	27	-8.8	–

[a] p: photographic, V: V-band, b: blue, v: visual
[b] first value for the blue part, second for the red part (see the text)

Plotting α, FWHM and W_λ versus a common parameter also allows us to easily extract information on their respective relations. For example, we find that α and W_λ show the expected roughly inverse relationship (with the exception of the extreme 'hybrid' α system V2104 Oph). We furthermore find our above suspicion confirmed that in spite of its faintness V693 CrA still inhabits an intrinsically bright accretion disc, as evidenced by its weak emission lines, and that the former is mainly due to the system seen at high i, as indicated by then line's width. On the other hand, V1370 Aql appears to be a low $\dot{M}$ system seen approximately face-on, as is suggested by its faint $M_{\min}$, low FWHM and strong W_λ.

5 SUMMARY

We have presented the recovery of five post-nova CVs with previously uncertain or unknown identifications. The candidates have been selected via *UBVR* photometry and confirmed spectroscopically. We furthermore have included first or improved spectroscopic data for another eight objects. With this we have further increased the number of confirmed post-novae. However, about 2/3 of the roughly 150 southern novae that were reported before 1980 still lack spectroscopic confirmation or even an identification of candidates for the post-nova, and there is thus still a long way to go until the post-novae make up a sample of statistical significance.

While the establishing of such a sample represents the main purpose of our project, we additionally find a number of systems that show peculiar properties that make them deserving of further, more detailed, investigation. Perhaps the most remarkable system in the present collection is X Cir. The profiles of the emission lines suggest that the hydrogen and He I lines form in the outer, cooler, parts of the accretion disc, with an additional component affecting the line profiles more (H) or less (He I) from possibly an irradiated secondary or a bright spot. On the other hand, the He II and carbon lines will originate in a more confined high-temperature region that does not allow for double peaks. Such could be either the innermost parts of the accretion disc, or, if X Cir should turn out to be an intermediate polar, the impact region of the gas stream on the surface of the white dwarf. The distinctively double-peaked HeI lines indicate a comparatively high system inclination. This suggests that the orbital period should be accessible by the means of time series photometry. On the other hand, high-resolved spectroscopic time series would be desirable to clarify the origin of the additional emission components, but such endeavour will be difficult due to the faintness of the object.

We have derived a number of parameters and investigated possible relations between them in order to gain information especially on the accretion state and the system inclination. Most of the systems included here appear to drive a high mass-transfer rate and/or are seen at comparatively low inclinations. However, X Cir and V693 CrA have broad emission lines that suggest a higher inclination. Their orbital period could thus be comparatively easily accessible via time series photometry, such as has been already performed successfully for the two novae with similar broad emission lines, V500 Cyg and V697 Sco (Haefner 1999; Warner & Woudt 2002, respectively). Furthermore, V356 Aql, V500 Aql, V1370 Aql and X Cir show comparatively strong emission lines and flat continuum slopes that indicates a lower mass-transfer rate than for other post-novae. Those systems could harbour instable accretion discs that allow for outburst-like behaviour (Honeycutt, Robertson, & Turner 1995, 1998; Tappert et al. 2013a) and thus may be worth of long-term photometric monitoring.

ACKNOWLEDGEMENTS

Thanks to Brian Skiff for bringing to our attention a couple of mistakes contained in the first arXiv upload.

We are indebted to the ESO astronomers who performed the service observations of the VLT data.

Many thanks to Antonio Bianchini and Elena Mason for interesting discussions especially concerning X Cir.

This research was supported by FONDECYT Regular grant 1120338 (CT and NV). AE acknowledges support by the Spanish Plan Nacional de Astrononomía y Astrofísica under grant AYA2011-29517-C03-01.

We gratefully acknowledge ample use of the SIMBAD data base, operated at CDS, Strasbourg, France, and of NASA's Astrophysics Data System Bibliographic Services. IRAF is distributed by the National Optical Astronomy Observatories. We thank the providers and maintainers of OpenSuSE and Ubuntu Linux operating systems.

REFERENCES

Appenzeller I. et al., 1998, The Messenger, 94, 1
Becker F., 1929, Astronomische Nachrichten, 237, 71
Becker F., 1930, Zeitschr. für Astroph., 1, 66
Bertaud C., 1947, Journal des Observateurs, 30, 1
Bessell M. S., 1990, PASP, 102, 1181
Burwell C. G., 1974, IAU Circ., 1092, 1
Campos J., Sanchez A., 1987, Information Bulletin on Variable Stars, 3030, 1
Cannon A. J., 1930, Harvard College Observatory Bulletin, 872, 1
Capaccioli M., della Valle M., D'Onofrio M., Rosino L., 1990, ApJ, 360, 63
Cardelli J. A., Clayton G. C., Mathis J. S., 1989, ApJ, 345, 245
Cohen J. G., 1985, ApJ, 292, 90
Collazzi A. C., Schaefer B. E., Xiao L., Pagnotta A., Kroll P., Löchel K., Henden A. A., 2009, AJ, 138, 1846
della Valle M., Livio M., 1995, ApJ, 452, 704
Downen L. N., Iliadis C., José J., Starrfield S., 2013, ApJ, 762, 105
Downes R. A., Duerbeck H. W., 2000, AJ, 120, 2007
Downes R. A., Webbink R. F., Shara M. M., Ritter H., Kolb U., Duerbeck H. W., 2005, Journal of Astronomical Data, 11, 2
Duerbeck H. W., 1987, Space Sci. Rev., 45, 1
Duerbeck H. W., Seitter W. C., 1987, Astroph. & Space Sci., 131, 467
Eckert W., Hofstadt D., Melnick J., 1989, The Messenger, 57, 66
Haefner R., 1999, Information Bulletin on Variable Stars, 4706, 1
Haefner R., 2004, Information Bulletin on Variable Stars, 5550, 1
Haefner R., Fiedler A., 2007, Information Bulletin on Variable Stars, 5751, 1
Honeycutt R. K., Robertson J. W., Turner G. W., 1995, ApJ, 446, 838
Honeycutt R. K., Robertson J. W., Turner G. W., 1998, AJ, 115, 2527
Horne K., 1986, PASP, 98, 609
Huth H., 1976, Information Bulletin on Variable Stars, 1205, 1
Johnson C. B., Schaefer B. E., Kroll P., Henden A. A., 2014, ApJ, 780, L25
Kosai H., Honda M., Nishimura S., Ando Y., Okazaki A., Mattei J., Collins P., Morgan J., 1982, IAU Circ., 3661, 1
Kozai Y., Kosai H., Honda M., Cragg T., 1981, IAU Circ., 3590, 1
Landolt A. U., 1983, AJ, 88, 439
Landolt A. U., 1992, AJ, 104, 340
Livio M., 1992, ApJ, 393, 516
Mason E., Howell S. B., 2003, A&A, 403, 699
Mayall M. W., 1946, Harvard College Observatory Bulletin, 918, 1
McLaughlin D. B., 1955, ApJ, 122, 417
Morel M., 1987, Information Bulletin on Variable Stars, 3096, 1
Osawa K., Kuwano V., 1976, IAU Circ., 2994, 1
Patterson J., 1984, ApJS, 54, 443
Patterson J. et al., 2013, MNRAS, 434, 1902
Ringwald F. A., Naylor T., Mukai K., 1996, MNRAS, 281, 192
Ritter H., Kolb U., 2003, A&A, 404, 301
Robertson J. W., Honeycutt R. K., Hillwig T., Jurcevic J. S., Henden A. A., 2000, AJ, 119, 1365
Robinson E. L., 1975, AJ, 80, 515
Rodríguez-Gil P. et al., 2007, MNRAS, 377, 1747
Rosino L., Iijima T., Ortolani S., 1983, MNRAS, 205, 1069
Saito R. K. et al., 2013, A&A, 554, A123
Schlafly E. F., Finkbeiner D. P., 2011, ApJ, 737, 103
Schlegel E. M., Honeycutt R. K., Kaitchuck R. H., 1985, PASP, 97, 1075
Schlegel D. J., Finkbeiner D. P., Davis M., 1998, ApJ, 500, 525
Schmidtobreick L., Tappert C., Bianchini A., Mennickent R., 2002, in American Institute of Physics Conference Series, Vol. 637, Classical Nova Explosions, Hernanz M., José J., eds., p.527
Schmidtobreick L., Tappert C., Bianchini A., Mennickent R. E., 2003, A&A, 410, 943
Schmidtobreick L., Tappert C., Bianchini A., Mennickent R. E., 2005, A&A, 432, 199
Shara M. M., Livio M., Moffat A. F. J., Orio M., 1986, ApJ, 311, 163
Smits D. P., 1991, MNRAS, 248, 20
Snijders M. A. J., Batt T. J., Roche P. F., Seaton M. J., Morton D. C., Spoelstra T. A. T., Blades J. C., 1987, MNRAS, 228, 329
Stetson P. B., 1992, in Astronomical Society of the Pacific Conference Series, Vol. 25, Astronomical Data Analysis Software and Systems I, Worrall D. M., Biemesderfer C., Barnes J., eds., p. 297
Strömgren E., 1936, Astronomische Nachrichten, 260, 375
Strope R. J., Schaefer B. E., Henden A. A., 2010, AJ, 140, 34
Szkody P., 1994, AJ, 108, 639
Tappert C., Bianchini A., 2003, A&A, 401, 1101
Tappert C., Ederoclite A., Mennickent R. E., Schmidtobreick L., Vogt N., 2012, MNRAS, 423, 2476
Tappert C., Vogt N., Schmidtobreick L., Ederoclite A., Vanderbeke J., 2013a, MNRAS, 431, 92
Tappert C., Schmidtobreick L., Vogt N., Ederoclite A., 2013b, MNRAS, 436, 2412
Thorstensen J. R., Ringwald F. A., Wade R. A., Schmidt G. D., Norsworthy J. E., 1991, AJ, 102, 272
Townsley D. M., Bildsten L., 2005, ApJ, 628, 395
Vanlandingham K. M., Starrfield S., Shore S. N., 1997, MNRAS, 290, 87
Vogt N., Krzeminski W., Sterken C., 1980, A&A, 85, 106
Wakuda M., 1983, IAU Circ., 3777, 1
Walton M. L., 1930, Harvard College Observatory Bulletin, 878, 8
Warmels R. H., 1992, in Astronomical Society of the Pacific Conference Series, Vol. 25, Astronomical Data Analysis Software and Systems I, Worrall D. M., Biemesderfer C., Barnes J., eds., p. 115
Warner B., Woudt P. A., 2002, PASP, 114, 1222
Wenzel W., 1992, Information Bulletin on Variable Stars, 3816, 1
Wild P., 1954, IAU Circ., 1471, 1
Williams G., 1983, ApJS, 53, 523
Williams R. E., Ney E. P., Sparks W. M., Starrfield S. G., Wyckoff S., Truran J. W., 1985, MNRAS, 212, 753
Woudt P. A., Warner B., 2002, in American Institute of Physics Conference Series, Vol. 637, Classical Nova Explosions, Hernanz M., José J., eds., p. 532
Woudt P. A., Warner B., Pretorius M. L., 2004, MNRAS, 351, 1015
Zacharias N. et al., 2010, AJ, 139, 2184
Zacharias N., Finch C. T., Girard T. M., Henden A., Bartlett J. L., Monet D. G., Zacharias M. I., 2013, AJ, 145, 44

APPENDIX A: FINDING CHARTS

We present the finding charts for the novae with previously ambiguous or unknown positions. The images correspond to the photometric R-band data from Table 3, but for V693 CrA, where the V-band data was used that had been analysed in Schmidtobreick et al. (2002). A finding chart for MT Cen can be found in Paper I. The other systems can be unambiguously identified from the charts presented by Downes et al. (2005). The nova MU Ser represents the only exception. While its position is marked in the finding chart of Duerbeck (1987), the object itself is not visible on that chart. The one by Downes et al. (2005) does not identify the nova either, but only marks a certain area. Since the acquisition frames of our spectroscopic data are lost, it falls to future photometric studies to provide a proper finding chart.

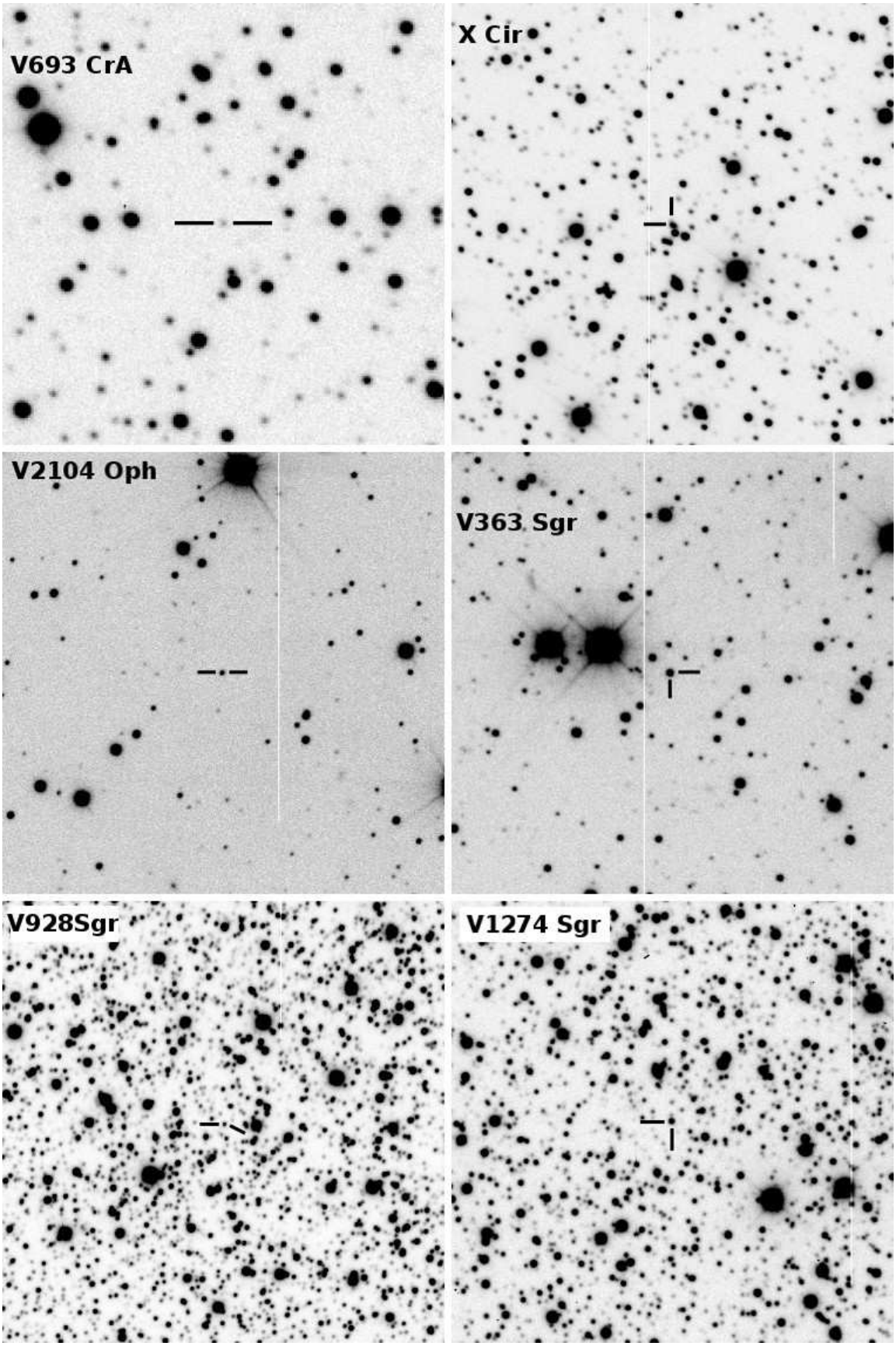

Figure A1. Finding charts for the recovered old novae as labelled. The size of a chart is 1.5×1.5 arcmin^2, and the orientation is such that north is up and east is to the left.